European Journal of Pharmaceutics and Biopharmaceutics 76 (2010) 376–383

Contents lists available at ScienceDirect

European Journal of Pharmaceutics and Biopharmaceutics

journal homepage: www.elsevier.com/locate/ejpb

Research paper

Chitosan hollow nanospheres fabricated from biodegradable poly-D,L-lactide-poly(ethylene glycol) nanoparticle templates

Weijia Wang [a], Chao Luo [b], Shijun Shao [b], Shaobing Zhou [a,b,*]

[a] School of Materials Science and Engineering, Key Laboratory of Advanced Technologies of Material, Southwest Jiaotong University, Chengdou, PR China
[b] School of Materials Science and Engineering, Southwest Jiaotong University, Chengdou, PR China

ARTICLE INFO

Article history:
Received 30 May 2010
Accepted in revised form 27 August 2010
Available online 9 September 2010

Keywords:
Hollow nanospheres
Biodegradable
Core-coated
Nanomedicine

ABSTRACT

Biodegradable chitosan hollow nanospheres were fabricated by employing uniform poly-D,L-lactide-poly(ethylene glycol) (PELA) nanoparticles as templates. Chitosan was adsorbed onto the surface of PELA nanoparticle templates through the electrostatic interaction between the sulphuric acid groups from sodium dodecyl sulfate (SDS) on the templates and the amino groups of the chitosan. Subsequently, the core-coated structure of chitosan–PELA nanospheres was obtained with the adsorbed chitosan layer being further crosslinked with glutaraldehyde. After the removal of the templates, PELA cores, chitosan hollow nanospheres were achieved. The mean size and size distribution of these nanospheres were measured with dynamic light scattering. The hollow structure was identified by transmission electron microscopy, atomic force microscopy and laser confocal scanning microscope. The antitumor drug model, adriamycin hydrochloride, was adsorbed on/into the chitosan hollow nanospheres. The drug release behaviors were investigated in phosphate buffered solution (PBS) at pH 7.4 and acetate buffered solution (ABS) at pH 4.5, respectively, at 37 °C, and in vitro tumor cell growth inhibition assay was also evaluated. The biodegradable hollow nanospheres possess great potential applications in nanomedicine.

1. Introduction

Hollow spheres have great potential for promising applications because of low effective density, high specific surface area and many other advantageous properties [1]. Especially, in recent years, hollow nanospheres have attracted considerable attention, because of their wide applications such as optical, electronic, magnetic and controlled drug-delivery carriers [2–4].

To date, there are various methods employed to prepare hollow spheres [3,5,6]. Some common methods are used to obtain hollow spheres, such as self-assembly of block copolymers [7–9], emulsion polymerization [10,11] and templates polymerization [12,13]. There are many ways for preparing hollow polymeric spheres [14–17], but the template method is often used, which can control the core size by selecting appropriate templates. After removing the template by dissolution, evaporation or thermolysis, hollow structures can be easily obtained. In this method, it required large amount of surfactants, which can modify the surface of the template to make the template active to interact with shell substance. Several research groups have developed some ways to change the surface character of templates, such as copolymerizing with some monomers to introduce active groups on the template surface [18], appending another special substance to adsorb polymer or monomers on the surface of templates [19–22] and directly modifying the templates through some chemical reaction [23]. Li et al. used sulfonated polystyrene (PS) microspheres as templates to prepare hollow spheres [24]. Generally, drug loaded with particles can be achieved mainly through two methods: (a) during the preparation of particles, (b) after the formation of particles. In hollow nanosphere system, drug is loaded after the formation of particles, and thus, the aqueous/organic interface produced by water-in-oil microemulsion and the acute shearing strength brought by a high-speed homogenizer caused drug like biomacromolecules denaturation, and aggregation could be avoided, which is an advantage compared to non-hollow nanoparticles [25].

However, the polymer matrix of most of the hollow spheres is nonbiodegradable, which limits their application in the field of drug delivery. In this study, chitosan (CS) was employed as the matrix of the hollow structure. The amino group in chitosan has a p*K*a value of 6.5; thus, chitosan is soluble in acidic solution and positively charged which readily binds to negatively charged surfaces. It has excellent biocompatibility and has been widely used in medicine, especially in gene delivery [20,26,27]. The template method was used to fabricate the CS hollow nanospheres. The surfactant, sodium dodecyl sulfate (SDS), was employed to enhance negative charge on the surface of PELA nanoparticle templates.

* Corresponding author at. School of Materials Science and Engineering, Southwest Jiaotong University, Chengdou 610031, Sichuan, PR China. Tel.: +86 28 87634023; fax: +86 28 87634649.
E-mail addresses: shaobingzhou@swjtu.cn, shaobingzhou@hotmail.com (S. Zhou).

0939-6411/$ - see front matter © 2010 Elsevier B.V. All rights reserved.
doi:10.1016/j.ejpb.2010.08.009

Using the PELA nanospheres as core template, CS shell can be formed easily by electrostatic force. The chitosan hollow spheres can be readily produced by removal of the PELA cores with acetone. Adriamycin, an anticancer drug with fluorescent properties, was adsorbed on/into these hollow nanospheres. The in vitro drug release from these hollow nanospheres was investigated in a medium with various pH values at 37 °C, and in vitro tumor cell growth inhibition assay was further evaluated.

2. Experimental

2.1. Materials

Poly-D,L-lactide-poly(ethylene glycol) (PELA) copolymers with PEG weight ratios of 10%, 15% and 30% and molecular weight (Mw) of 4 kDa were synthesized by ring-opening polymerization in our laboratory [28]. The Mw of PEG and PLA in PELA with PEG ratios of 10%, 15% and 30% is 4500 and 26,500, 6400 and 16,700, 10,900 and 4100 g mol^{-1}, respectively, determined by gel permeation chromatograph (GPC, Waters ALC/GPC 244, USA) using polystyrene as standards. Chitosan was obtained from Yuhuan Ocean Biochemical Co. Ltd., China. Its degree of deacetylation and viscosity molecular weight were 95% and 7.57×10^5, respectively. Polyvinyl alcohol (PVA, M_n of 130,000 g mol^{-1}, degree of hydrolysis 88) was purchased from Shanghai Petrochemical Industry Company (China). 3-(4,5-Dimethylthiazol-2-yl)-2,5-diphenyltetrazolium bromide (MTT) was purchased from Sigma. HepG2 tumor cells were also purchased from the American Type Culture Collection (ATCC; Rockville, MD, USA). Adriamycin hydrochloride was purchased from Zhejiang Hisun Pharmaceutical Co., Ltd. (China). Fluorescein isothiocyanate (FITC) was purchased from Sigma–Aldrich Inc. (St. Louis, MO). All the chemicals used in this research were the analytical reagent grade from the commercial market without further purification.

2.2. Fabrications of PELA nanoparticles as templates

PELA nanoparticles were prepared by single emulsion method (O/W) based on solvent evaporation [28,29]. First, 0.2 g polymer was dissolved in 5 mL acetone and mixed with span 80 as surfactant under stirring, formed the stable organic phase (O). Secondly, the resultant solution was added dropwise into 50 mL of 20% (w/v) PEG aqueous solution (W) and emulsified for 40 min using overhead stirrer from 900 to 1400 rpm. Finally, the solution was stirred about 2 h in fuming cupboard. After the solvent evaporated completely, the nanoparticles were collected by centrifuge (Avanti TM J-30I, BECKMAN COULTER, USA) for 15 min at 20,000 rpm. The resultant nanoparticles were rinsed three times with distilled water and centrifuged three more times. Followed this, the slurry of the nanoparticles was dispersed in 10 mL SDS solution (1.0%) and stirred gently for 2 h. After that, the emulsion of the nanoparticles was centrifuged again for removing redundant SDS. Thus, the SDS coated nanoparticles were gained.

2.3. Preparation of core–shell CS–PELA nanospheres

FITC-labeled CS aqueous solution was prepared as follows. Briefly, preweighed CS was first dissolved in 0.1 mol/L acetic acid solution, and then 1.5% CS solution was obtained by adding distilled water. Finally, the CS solution was mixed with FITC (FITC/CS: 1/50) under stirring for 12–14 h at 0–4 °C. The FITC-labeled CS was gained.

0.2 g SDS coated nanospheres were dispersed in 10 mL FITC-labeled CS aqueous solution and subsequently stirred gently for about 12 h. The resultant nanospheres were centrifuged to remove unnecessary CS. The CS absorbed PELA nanospheres were re-dispersed in 10 mL of 2.0% glutaraldehyde (GA) aqueous solution as the cross-linker [30] under gentle stirring for about 30 min to further solidify the CS layer on the surface of PELA nanospheres. The resultant nanospheres were rinsed with distilled water and centrifuged three more times, then lyophilized overnight. Thus, the CS–PELA nanospheres were obtained.

2.4. Preparation of adriamycin-loaded CS hollow nanospheres

The CS–PELA nanospheres were dispersed in acetone and stirred gently for 4 h. After the PELA cores were dissolved completely, the solution was first centrifuged. Later, the resultant hollow nanospheres were re-dispersed in aqueous and rinsed with distilled water and centrifuged three more times, finally lyophilized overnight.

The hollow nanospheres (200 mg) were dispersed in 1 mL adriamycin aqueous solution and gently shook for 2 h. The adriamycin-loaded hollow nanospheres were recollected by centrifugation and lyophilized overnight and stored at 4 °C in a desiccator. The adriamycin concentration in the supernatant was detected by UV–visible spectrophotometer (UV-2550, Shimadzu, Japan). The loading amount of adriamycin encapsulated into nanospheres was calculated using following equation [31]:

$$q = \frac{(c_i - c_f)V}{m} \quad (1)$$

where c_i is the initial adriamycin solution concentration, and c_f is the adriamycin concentration of supernatant after centrifuge. V is the total volume of adriamycin solution. And m is the weight of the CS hollow nanospheres.

2.5. Characterization of the particles

The mean size, size distribution and the zeta potential of the nanoparticles dispersed in water medium were determined by dynamic light scattering (DLS) using a ZETA-SIZER, MALVERN Nano-ZS90 (Malvern Ltd., Malvern, UK). Each measurement was repeated three times, and an average value reported.

The morphology of the core-coated and CS hollow nanospheres was examined by scanning electron microscope (SEM, QUANTA 200, FEI, USA). Several solution droplets containing these nanospheres were placed on the SEM sample stage. The samples were sputter coated with gold after lyophilized overnight.

To observe the core–shell and hollow structure of the nanospheres, transmission electron microscopy observation was further performed with a HITACHI H-700H (TEM, Japan) at the acceleration voltage of 150 kV and laser confocal scanning microscope (LCSM, Leica TCS SP2, Germany). The samples of TEM were prepared by dropping the nanospheres suspension on a carbon-coated copper grid and then air-dried before measurement. Herein, both the FITC-labeled and adriamycin-loaded CS hollow nanospheres were observed with LCSM. Excitation and emission wavelengths of FITC were 488 and 535 nm, respectively, and those of adriamycin were 480 and 590 nm, respectively.

The morphology of the particles in aqueous was also examined by tapping-mode atomic force microscopy (AFM) measurements (CSPM5000, Beijing, China). The AFM sample was prepared by casting a dilute particle solution on a slid silicon piece, which was then dried under vacuum.

2.6. In vitro drug release

Preweighed nanospheres (0.1 g) were suspended in a test tube containing 10 mL phosphate buffered solution (PBS) at pH 7.4 and acetate buffered solution (ABS) at pH 4.5, respectively. The tubes were kept in a thermostated incubator (Haerbin Dongming

Medical Equipment Company, China) which was maintained at 37 °C and 100 cycles per minute. At predetermined intervals, 1.0 mL of supernatant was collected by centrifuge, and 1.0 mL of fresh PBS and ABS were added into the test tube. Concentration of adriamycin released was determined by UV–visible spectrophotometer at absorbance of 232 nm.

2.7. In vitro tumor cell growth inhibition assay

HepG2 cells were cultured in RPMI 1640 medium supplemented with 10% fetal bovine serum (FBS) at 37 °C in a 5% CO_2 incubator. The tumor cells were planted at a density of 1×10^4 cells per well in 100 μL of medium and grown in 96-well plates, into which the suitable slides were put. The cells were then exposed to a series of adriamycin-loaded hollow nanoparticles at different concentrations for 48 h, and free adriamycin solution with the same concentration was used as control. Finally, viability of cells was measured using the methyl thiazolyl tetrazolium (MTT) assay. All data were expressed as the mean ± SD. Cell viability was determined by the following formula:

$$\text{Cell viability } (\%) = \frac{\text{OD (test well)}}{\text{OD (reference well)}} \times 100\% \quad (2)$$

The data were estimated from six individual experiments, and all data were expressed as the mean ± SD.

Optical microscopy (OM) was performed to observe the cell morphology and endocytosis of nanoparticles under the adriamycin concentration of 2 μg/mL, 8 μg/mL and 16 μg/mL. Before fluorescence microscopy observation, the samples were washed three times for removing un-endocytosis drug. Finally, through the paraformaldehyde and ethanol fixative, the cells were fixed in slides to be observed by optical/fluorescence microscopy.

2.8. Cell viability by MTT assay

HepG2 tumor cells were also grown in RPMI medium 1640 with 10% FBS. The tumor cells were seeded at a density of 1×10^4 cells per well in 1.5 mL of medium in 12-well plates and grown for 12 h. The cells were then exposed to adriamycin-loaded hollow nanospheres group and hollow CS nanospheres group at same concentrations (10 μg/mL) for 72 h, and hollow CS nanospheres were used as control. Cell viability was measured using the MTT method. The data were estimated from six individual experiments, and all data were expressed as the mean ± SD.

2.9. Statistics

Statistical analysis was performed using SPSS version 13.0. ANOVA was used to analyze statistical comparisons between groups. The level of significance was set at $p < 0.05$.

3. Results and discussion

3.1. Characterization of PELA nanoparticle templates

PELA nanoparticles were selected as templates as previously reported [24]. First, the experiment parameters to influence the size of PELA nanoparticles should be investigated. Here, the experiment parameters were studied, including the stirring speeds, the proportion of the solvent to water, the content of PEG in PELA backbone, the concentration of SDS as a surfactant (Table 1). Through the optimization of experiment parameters (stirring speeds: 1200 rpm; the proportion of the solvent to water: 1:2; content of PEG in PELA copolymer: 15%; concentration of SDS: 0.1%), the mean size of PELA template was gained, which was 180 ± 2 nm, and the polydispersity (Pdi) was 0.09 that demonstrated the size of nanospheres was almost uniform.

Table 1
Optimization of the experiment parameters to fabricate PELA nanoparticles.

Experiment parameters[a]		Size ± SD (nm)	Pdi
Stirring speed (rpm)	900	280 ± 7	0.13
	1000	272 ± 13	0.19
	1200	259 ± 10	0.31
	1400	239 ± 15	0.22
$V_{solvent}$:V_{water}	1:1	134 ± 13	0.27
	1:2	152 ± 17	0.24
	1:5	168 ± 10	0.18
	1:10	189 ± 8	0.13
PEG content	10%	197 ± 7	0.11
	15%	162 ± 10	0.11
	30%	145 ± 9	0.43
SDS (wt.%)	0	146 ± 5	0.20
	0.01	152 ± 3	0.15
	0.02	171 ± 6	0.13
	0.04	183 ± 3	0.11
	0.1	180 ± 2	0.09
	0.3	185 ± 3	0.14
	0.5	187 ± 2	0.2

[a] The experiment parameters include: the stirring speeds, the ratio of the organic solvent and water, the content of PEG in PELA copolymer and the content of the SDS surfactant.

3.2. Characterization of hollow CS nanospheres

The build-up of shell of the nanospheres was accompanied by an increase in particle size, as determined by DLS. The mean size of initial PELA nanospheres was 180 ± 2 nm versus 280 ± 12 nm for CS–PELA nanospheres, and the zeta potential changed from −31.5 to 41.3 mV (shown in Fig. 1b). The change of zeta potential and size were noteworthy, which indicated that CS was adsorbed on the surface of PELA nanospheres. Thus, it is possible to form the hollow CS nanospheres by removing the PELA core.

Fig. 2 displays the typical TEM (A and B), SEM (C and D) and AFM (E–G) images of these nanospheres. From Fig. 2A and B corresponding to the CS–PELA core–shell nanospheres and the hollow CS nanospheres, separately, we can see that the nanospheres took a good dispersion and all were well sphere shaped. The core–shell structure was one of the most important properties for hollow CS nanospheres in this study. Thus, through observing the TEM photographs in Fig. 2A, we could find that the core–shell structure is very clear due to the different kinds of materials presented in core and shell layer. The color of inner core is darker than that of coated layer. The reason is that the core, PELA nanosphere, is solid whereas the shell, CS gel, is transparent. Fig. 2B confirmed that the nanospheres have hollow structure. The SEM photographs of the hollow nanospheres before and after ultrasonication were displayed in Fig. 2C and D, respectively. Before broken, a well sphere shaped was observed, and the hollow structure of nanospheres could be seen after ultrasonication, especially inserted magnification photograph displaying the interior hollow structure. Seen from the AFM 3D photographs of the bare (Fig. 2E) and hollow nanospheres before (Fig. 2F) and after (Fig. 2G) ultrasonication, the hollow structure could be further confirmed. Therefore, based on above results we could draw a conclusion that the hollow CS nanospheres were achieved.

3.3. Encapsulation of drug into hollow CS nanospheres

Adriamycin is a commonly used chemotherapeutic drug in the treatment of hepatocellular carcinoma [32]. In the study, drug

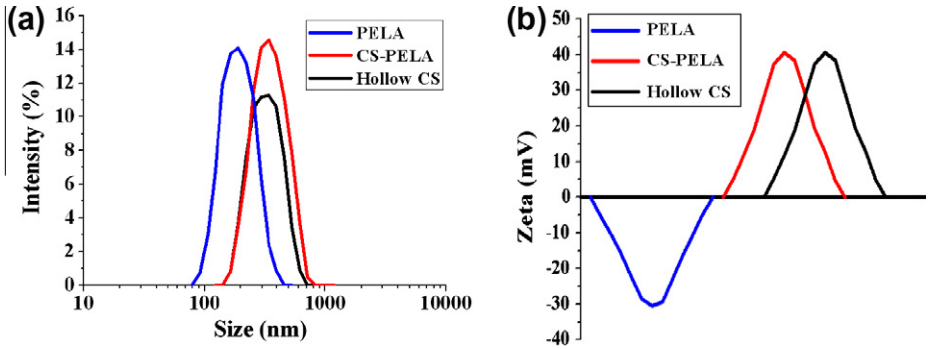

Fig. 1. Average particle size and distribution (a) and the zeta potential (b). Values are reported as mean ± standard error. (For interpretation of the references to color in this figure legend, the reader is referred to the web version of this article.)

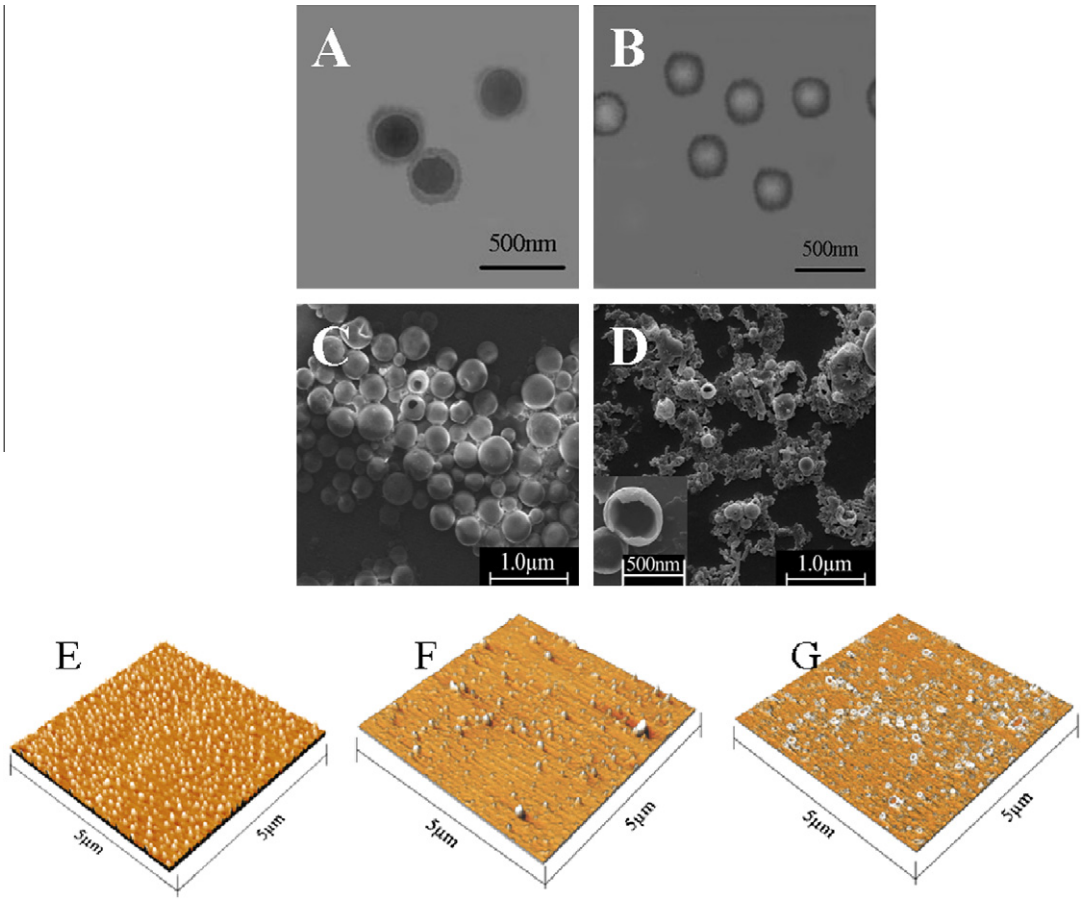

Fig. 2. The morphology of the core–shell CS–PELA nanospheres (A), and hollow CS nanospheres (B) detected by TEM, the hollow nanospheres before (C) and after (D) ultrasonication detected by SEM, and PELA template (E) and hollow nanospheres before (F) and after (G) ultrasonication detected by AFM. (For interpretation of the references to color in this figure legend, the reader is referred to the web version of this article.)

loading was performed through drug diffusing into the hollow nanospheres [21]. Hollow nanospheres were physically embedded into the drug solution with different concentration under the different temperature. Drug penetrated into the interior of hollow CS nanospheres by diffusion because of the difference of drug concentration between inside and outside of the hollow nanospheres. Herein, the diffusion of drug may be considered as adsorption of drug into hollow nanospheres, which is an equilibrium process. In order to obtain the high loading amount of drug in nanospheres, it is very necessary to investigate the effects of some important parameters on it. Fig. 3 displays the effects of different concentrations and time (A) and temperature (B) on drug adsorbing efficiency. The effect of temperature was reported in our previous research [31]. It indicated that the temperature had a slight effect on adsorbing efficiency, which was consistent with the study. Adriamycin adsorption was carried out at 25 °C in this research, which was a mild condition for keeping drug biological activity. As shown in Fig. 3A, the adsorption amount almost reached the peak and kept a stable value after 2 h adsorption when the adriamycin concentration was 4 mg/mL. The adsorption efficiency is about 80%, which is higher than previous reports [33], and the drug loading amount is 1.1% (w/w). These indicated that the adsorption of adriamycin into hollow CS nanospheres had got to an equilibrium under these conditions: the adsorption time is greater than

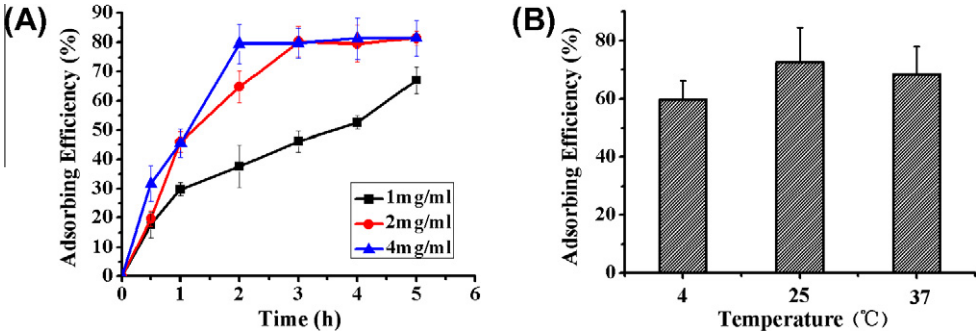

Fig. 3. The effects of CS nanosphere concentration and time (A) and temperature (B) on drug adsorbing efficiency. (For interpretation of the references to color in this figure legend, the reader is referred to the web version of this article.)

or equal to 2 h, adriamycin concentration is 4 mg/mL, and the temperature is 25 °C. As the SEM and TEM images cannot provide evidences that adriamycin was successfully encapsulated inside the hollow nanospheres, several means to characterize the encapsulation profiles were employed. Chitosan was labeled with FITC, the hollow nanospheres and adriamycin-loaded hollow nanospheres were observed under LCSM. Fig. 4A shows that the hollow nanospheres emitted green light, suggesting the presence of hollow structure. Fig. 4B shows that the hollow nanospheres emitted green light and adriamycin emitted red light, suggesting that adriamycin was successfully encapsulated. Most importantly, in our system, the drug in hollow nanospheres could maintain its original molecular structure by the adsorption of drug. Therefore, the system is potentially suitable for entrapping biomacromolecule drugs such as protein and polypeptide.

3.4. In vitro drug release

Fig. 5 displays the percent release of adriamycin from the hollow nanospheres incubated in PBS at pH 7.4 and ABS at pH 4.5, respectively, at 37 °C. Fig. 5 shows that 70% of adriamycin was released in ABS at first 20 h while 20% of adriamycin was released from the nanospheres in PBS. The adriamycin release profiles occur in a biphasic manner: an initial fast release phase and then leveling off. It is obvious that the release of the adriamycin was influenced by the pH values of the release medium. The release rate decreases with the increase in pH value of the release medium. The release profile presents a faster release rate at pH 4.5 than that at pH 7.4. This can be explained by the fact that the release of the adriamycin depends greatly on its pH-dependence and the swelling of the hollow nanospheres. As we know, the solubility of adriamycin in acid solution is better than that in neutral solution. Herein, the release mechanism of drug from the CS hollow nanospheres was mainly by drug diffusion. So adriamycin could be diffused into ABS more easily than that into PBS. Moreover, the hollow nanospheres can be swollen to a great extent at acidic condition because the amino groups of CS are destroyed, leading to the breaking of the strong hydrogen bonds between the CS chains

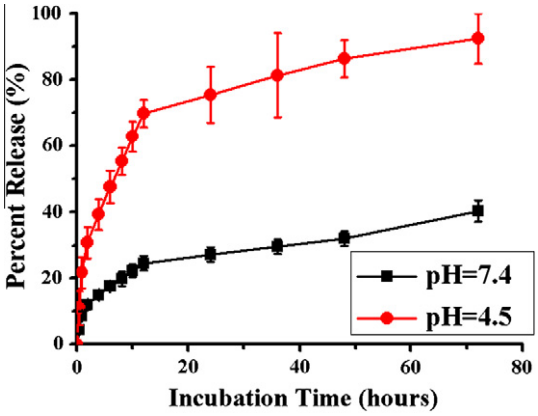

Fig. 5. Percent release of adriamycin from the hollow nanospheres incubated in PBS and ABS, respectively, at 37°. (For interpretation of the references to color in this figure legend, the reader is referred to the web version of this article.)

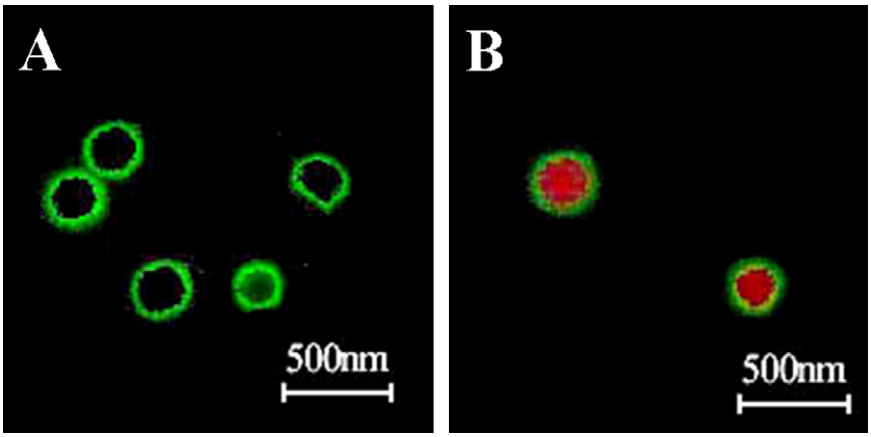

Fig. 4. The morphology of the hollow nanospheres detected by LCSM. Overview LCSM image of hollow nanospheres (A) and adriamycin-loaded hollow nanospheres (B). (For interpretation of the references to color in this figure legend, the reader is referred to the web version of this article.)

and resulting in a fairly faster release of adriamycin [24]. However, at high pH value, the nanospheres could be limitedly swelled. The adriamycin was entrapped into the hollow nanospheres and could not be released easily.

3.5. In vitro tumor cell growth inhibition assay

Following intravenous administration, polymeric particles were accumulated in tumor tissue by enhanced permeability and retention effect and then taken up to cells via endocytosis process [34,35]. The pH value of endosomal compartments was decreased from 7.4 to about 5 because protons are pumped into the vesicles [36]. In our system, the hollow structures can be stabilized to preserve adriamycin drug under physiological conditions (pH = 7.4) and selectively release the drug by sensing the intracellular pH change (pH 4–5).

The research about treatment of HepG2 cells by adriamycin has been reported [32]. The MTT assay was performed to evaluate whether adriamycin-loaded hollow CS nanospheres and free adriamycin had the same influence on cell growth [37]. Both adriamycin-loaded hollow CS nanospheres and free adriamycin at various concentrations significantly inhibited the growth of HepG2 cells. Fig. 6a displays when the drug concentration increased, the amount of cells reduced; when the drug concentration is same,

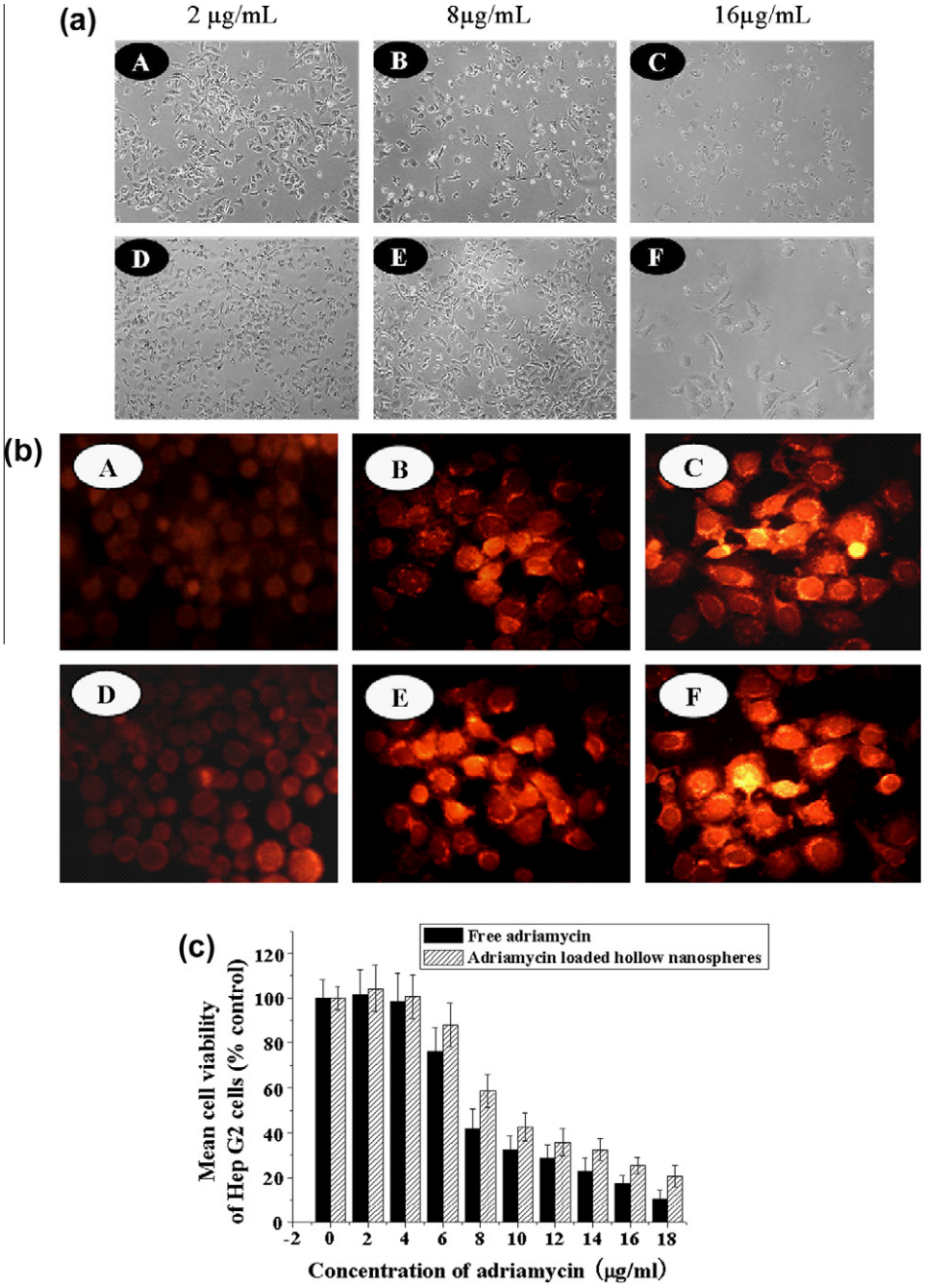

Fig. 6. (a) Optical microscopic observation (100×) and (b) fluorescent microscopy observation (200×) of HepG2 incubated with free adriamycin (A–C) and adriamycin-loaded hollow nanospheres (D–F) with the drug concentration of 2 μg/mL, 8 μg/mL and 16 μg/mL, and (c) the mean cell viability of HepG2 cells with 48 h by MTT assay under different drug concentration. Error bars represent the standard deviation (n = 6). (For interpretation of the references to color in this figure legend, the reader is referred to the web version of this article.)

e.g. 16 μg/mL, the cells in adriamycin-loaded hollow CS nanospheres group would be bigger than that in free adriamycin group. The reason may be the presence of chitosan leads to cell hypertrophy [38]. To investigate the intracellular uptake of the hollow nanospheres, we took a series of fluorescence micrographs after they were dispersed in the cell culture (Fig. 6b). The microscopic images were from HepG2 cells incubated with the concentration of adriamycin at 2 μg/mL, 8 μg/mL, and 16 μg/mL, respectively, for 24 h at 37 °C. The red inside the cells was produced from adriamycin fluorescence. It is obvious to be observed that the intensity of red fluorescence in tumor cells increased with the concentration of adriamycin increased, which indicates that both the free adriamycin and drug-loaded CS hollow nanospheres engulfed by cells increase with drug concentration increased. Fig. 6C presents the influence of drug concentration on cell viability of HepG2 cells. The result indicates that the cytotoxicity of the adriamycin-loaded hollow CS nanosphere is comparable to that of free adriamycin even though adriamycin was released in an extended behavior. The results of tumor cell growth were basically consistent with the control group in Fig. 6. Combining Fig. 5 with Fig. 6, we could get a conclusion that in the acidic environment of tumor cells, the hollow nanospheres played an important role in drug delivery, and drug effect is the same with the equivalent amount of free adriamycin.

3.6. Cell viability by MTT method

The cell viability, which was measured by MTT assay, is shown in Fig. 7. A group was blank group; B group was pristine hollow CS nanospheres used as control group, and C group was adriamycin-loaded hollow nanospheres group was used as experiment group. First, as the blank group (A group), the amount of cells could be gained under different hours. Later, compared with the data of blank group ($p < 0.05$), it could be found that the cell proliferation in B group was inhibited to a certain extent due to the existence of hollow CS nanospheres, but the cell viability still retained about 85% with prolonging the culture time. It has been reported that the hollow CS nanospheres had some cytotoxicity [39]. It was obvious that with the culture time increased, the tumor cell growth was inhibited in the C group. The reason may be that with the culture time increased, adriamycin was released from the nanospheres to inhibit the cell proliferation as shown in Fig. 6C. Combined with Figs. 5 and 6b, we could deem that the endocytosis of adriamycin-loaded hollow nanospheres was fulfilled, because when pH value was 7.4, there was only a small amount of drug released, whereas as the pH value decreased to less than 5.0 inside tumor cells, more amount of drug would be released.

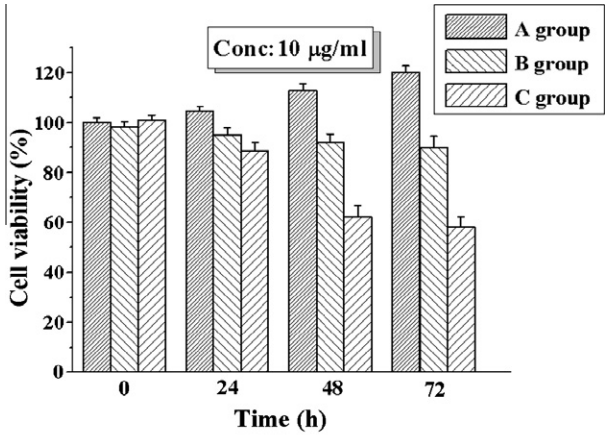

Fig. 7. The cell viability of HepG2 cells by MTT assay at different time. A group was blank group; B group was blank hollow CS nanospheres used as a control group; C group was adriamycin-loaded hollow nanospheres group. $p < 0.05$.

4. Conclusions

In this study, a template method was employed to fabricate biodegradable, biocompatible CS hollow nanospheres. PELA nanosphere template was prepared by single emulsion method (O/W) based on solvent evaporation, and the surfactant, SDS, was employed to improve negative charge on the surface of PELA templates. The core-coated nanospheres (CS–PELA) were fabricated by adsorbed CS on PELA nanoparticles, and the hollow nanospheres were obtained by removal of the PELA core. The TEM, SEM, LCSM and AFM photographs confirmed that the nanospheres had obvious hollow structure, and LCSM further demonstrated that the adriamycin could be successfully encapsulated into the hollow nanospheres. Furthermore, the release behavior in a medium with various pH values at 37 °C indicated that the pH value of the release medium played an important role during the release of the adriamycin. Finally, in vitro tumor cell growth inhibition assay was also investigated to prove the drug effect of the adriamycin-loaded hollow nanospheres is the same with the equivalent amount of free adriamycin. Therefore, the hollow nanospheres may have great potential for application as a nanocarrier in drug delivery system.

Acknowledgements

This work was partially supported by National Natural Science Foundation of China (30970723), Programs for New Century Excellent Talents in University, Ministry of Education of China (NCET-07-0719) and Sichuan Prominent Young Talent Program (08ZQ026-040).

References

[1] J. Bertling, J. Blömer, R. Kümmel, Template-free fabrication of porous zinc oxide hollow spheres and their enhanced photocatalytic performance, Chemical Engineering & Technology 27 (2004) 8290–8297.
[2] F. Caruso, RA. Caruso, H. Mohwald, Nanoengineering of inorganic and hybrid hollow spheres by colloidal templating, Science 282 (1998) 111–1114.
[3] P. Jiang, J.F. Bertone, V.L. Colvin, A lost-wax approach to monodisperse colloids and their crystals, Science 291 (2001) 453–457.
[4] J. Liu, Q.H. Yang, L. Zhang, Organic–inorganic hybrid hollow nanospheres with microwindows on the shell, Chemistry of Materials 20 (2008) 4268–4275.
[5] Y.H. Ni, R. Liu, X.F. Cao, X.W. Wei, J.M. Hong, Preparation and transformation to hollow nanospheres of wrapped CuS nanowires by a simple hydrothermal route, Materials Letters 61 (2007) 1986–1989.
[6] J. Han, GP. Song, R. Guo, A facile solution route for polymeric hollow spheres with controllable size, Advanced Materials 18 (2006) 3140–3144.
[7] J.W. Kim, Y.G. Joe, K.D. Suh, Poly(methyl methacrylate) hollow particles by water-in-oil-in-water emulsion polymerization, Colloid and Polymer Science 277 (1999) 252–256.
[8] S. Stewart, G.J. Liu, Hollow nanospheres from polyisoprene-block-poly(2-cinnamoylethyl methacrylate)-block-poly(tert-butyl acrylate), Chemistry of Materials 11 (1999) 1048–1054.
[9] K. Breitenkamp, T. Emrick, Novel polymer capsules from amphiphilic graft copolymers and cross-metathesis, Journal of the American Chemical Society 125 (2003) 12070–12071.
[10] Y. Yang, C. Ying, Y.P. Zhang, F.Y. Yang, J.L. Liu, Polystyrene–ZnO core–shell microspheres and hollow ZnO structures synthesized with the sulfonated polystyrene templates, Journal of Solid State Chemistry 179 (2006) 470–475.
[11] W.J. Liu, Z.C. Zhang, W.D. He, Novel one-step route for synthesizing submicrometer PSt hollow spheres via redox interfacial-initiated method in inversed emulsion, Materials Letters 61 (2007) 2818–2821.
[12] T.H. Kim, K.H. Lee, Y.K. Kwon, Monodisperse hollow titania nanospheres prepared using a cationic colloidal template, Journal of Colloid and Interface Science 304 (2006) 370–377.
[13] N. Singh, LA. Lyon, Au nanoparticle templated synthesis of pNIPAm nanogels, Chemistry of Materials 19 (2007) 719–726.
[14] V.N. Pavlyuchenko, O.V. Sorochinskaya, S.S. Ivanchev, V.V. Klubin, G.S. Kreichman, V.P. Budto, M. Skrifvars, E. Halme, J. Koskinen, Hollow-particle latexes: preparation and properties, Journal of Polymer Science Part A: Polymer Chemistry 39 (2001) 1435–1449.

[15] X. He, X. Ge, M. Wan, Z. Zhang, Morphology control of hollow polymer latex particle preparation, Journal of Applied Polymer Science 98 (2005) 860–863.
[16] G.D. Fu, J.P. Zhao, Y.M. Sun, E.T. Kang, K.G. Neoh, Conductive hollow nanospheres of polyaniline via surface-initiated atom transfer radical polymerization of 4-vinylaniline and oxidative graft copolymerization of aniline, Macromolecules 40 (2007) 2271–2275.
[17] W. Wu, D. Caruntu, A. Martin, Synthesis of magnetic hollow silica using polystyrene bead as a template, Journal of Magnetism and Magnetic Materials 311 (2007) 578–582.
[18] C. Barthet, S.P. Armes, S.F. Lascelles, S.Y. Luk, H. Stanley, Synthesis and characterization of micrometer-sized polyaniline-coated polystyrene latexes, Langmuir 14 (1998) 2032–2041.
[19] S.F. Lascelles, S.P. Armes, Synthesis and characterization of micrometre-sized, polypyrrole-coated polystyrene latexes, Journal of Materials Chemistry 7 (1997) 1339–1347.
[20] S.F. Lascelles, S.P. Armes, P.A. Zhdan, S.J. Greaves, A.M. Brown, J.F. Watts, S.R. Leadley, S.Y. Luk, Surface characterization of micrometre-sized, polypyrrole-coated polystyrene latexes: verification of a 'core–shell' morphology, Journal of Materials Chemistry 7 (1997) 1349–1355.
[21] B. Sarmento, A. Ribeiro, F. Veiga, P. Sampaio, R. Neufeld, D. Ferreira, Alginate/chitosan nanoparticles are effective for oral insulin delivery, Pharmaceutical Research 24 (2007) 2198–2206.
[22] L.Y. Wang, Y.H. Gu, Q.Z. Zhou, G.H. Ma, Preparation and characterization of uniform-sized chitosan micro spheres containing insulin by membrane emulsification and a two-step solidification process, Colloids and Surfaces B: Biointerfaces 50 (2006) 126–135.
[23] Y. Yang, Y. Chu, F.Y. Yang, Y.P. Zhang, Uniform hollow conductive polymer microspheres synthesized with the sulfonated polystyrene template, Materials Chemistry and Physics 92 (2005) 164–171.
[24] H.M. Li, M.Z. Wang, L.Y. Song, X.W. Ge, Uniform chitosan hollow microspheres prepared with the sulfonated polystyrene particles templates, Colloid and Polymer Science 286 (2008) 819–825.
[25] S.A. Agnihotri, N.N. Mallikarjuna, T.M. Aminabhvi, Recent advances on chitosan-based micro- and nanoparticles in drug delivery, Journal of Controlled Release 100 (2004) 25–28.
[26] G. Borchard, Chitosans for gene delivery, Advanced Drug Delivery Reviews 52 (2001) 145–150.
[27] A. Grenha, B. Seijo, C.R. Lopez, Microencapsulated chitosan nanoparticles for lung protein delivery, European Journal of Pharmaceutical Sciences 25 (2005) 427–437.
[28] X. Deng, S. Zhou, X. Li, J. Zhao, M. Yuan, In vitro degradation and release profiles for poly-D,L-lactide-poly(ethylene glycol) microspheres containing human serum albumin, Journal of Controlled Release 71 (2001) 165–173.
[29] Y. Yang, W. Jia, X. Qi, C. Yang, L. Liu, Z. Zhang, J. Ma, S. Zhou, X. Li, Novel biodegradable polymers as gene carriers, Macromolecular Bioscience 4 (2004) 1113–1117.
[30] W.J. Tong, C.Y. Gao, H. Mohwald, Manipulating the properties of polyelectrolyte microcapsules by glutaraldehyde cross-linking, Chemistry of Materials 17 (2005) 4610–4616.
[31] L. Sun, S. Zhou, W. Wang, X. Li, J. Wang, J. Weng, Preparation and characterization of porous biodegradable microspheres used for controlled protein delivery, Colloids and Surfaces A: Physicochemical Engineering Aspects 345 (2009) 173–181.
[32] H. Qian, Y. Yang, Alterations of cellular organelles in human liver-derived hepatoma G2 cells induced by adriamycin, Anticancer Drugs 20 (9) (2009) 779–786.
[33] R. Misra, S.K. Sahoo, Intracellular trafficking of nuclear localization signal conjugated nanoparticles for cancer therapy, European Journal of Pharmaceutical Science 39 (2010) 152–163.
[34] J. Daruwalla, K. Greish, C. Malcontenti-Wilson, V. Muralidharan, A. Iyer, H. Maeda, C. Christophi, Styrene maleic acid-pirarubicin disrupts tumor microcirculation and enhances the permeability of colorectal liver metastases, Journal of Vascular Research 46 (3) (2009) 218–228.
[35] Y.Y. Lin, J.J. Li, C.H. Chang, Y.C. Lu, J.J. Hwang, Y.L. Tseng, W.J. Lin, G. Ting, H.E. Wang, Evaluation of pharmacokinetics of 111in-labeled VNB-PEGylated liposomes after intraperitoneal and intravenous administration in a tumor/ascites mouse model, Cancer Biotherapy and Radiopharmaceuticals 24 (4) (2009) 453–460.
[36] W. Arap, R. Pasqualini, E. Ruoslahti, Cancer treatment by targeted drug delivery to tumor vasculature in a mouse model, Science 279 (1998) 377–380.
[37] C.Y. Gong, S. Shi, P.W. Dong, B. Kan, M.L. Gou, X.H. Wang, X.Y. Li, F. Luo, X. Zhao, Y.Q. Wei, Z.Y. Qian, Synthesis and characterization of PEG–PCL–PEG thermosensitive hydrogel, International Journal of Pharmaceutics 365 (2009) 89–99.
[38] F. Mwale, H.T. Wang, S. Lerouge, J. Antoniou, M.R. Wertheimer, Suppression of genes related to hypertrophy and osteogenesis in committed human mesenchymal stem cells cultured on novel nitrogen-rich plasma polymer coatings, Tissue Engineering 12 (9) (2006) 2639–2647.
[39] M. Huang, E. Khor, L. Lim, Uptake and cytotoxicity of chitosan molecules and nanoparticles: effects of molecular weight and degree of deacetylation, Pharmaceutical Research 21 (2004) 344–353.